Structural and photophysical investigations of polyacetylene prepared by different precursor routes

J. H. F. Martens, K. Pichler, E. A. Marseglia and R. H. Friend*
Cavendish Laboratory, University of Cambridge, Madingley Road, Cambridge CB3 0HE, UK

and H. Cramail, E. Khosravi, D. Parker and W. J. Feast
Department of Chemistry and Interdisciplinary Research Centre in Polymer Science and Technology, University of Durham, Durham DH1 3LE, UK
(Received 8 April 1993; revised 21 October 1993)

We report here structural and photophysical studies on polyacetylene prepared by various precursor routes. We find that control of stereoregularity, molecular weight and molecular weight distribution of the precursor allows improvements in ordering parameters, such as molecular orientation and crystallographic order of the final polymer. The photophysical properties of polyacetylene also depend on the particular precursor preparation route. The peak in the π–π^* absorption lies between 2.15 and 2.65 eV, depending on the precursor; also, photoinduced metastable band-gap states vary in position, shape and strength.

(Keywords: polyacetylene; structure; precursor)

INTRODUCTION

Polyacetylene is the simplest example of a conjugated polymer. It has therefore been the subject of many studies, and much of the understanding of conjugated polymers arises from investigations on this system. Polyacetylene was first available as a powder formed directly by polymerization of acetylene in solution in the presence of a $Ti(OBu)_4/AlEt_3$ catalyst[1]. Later Ito *et al.*[2] produced polyacetylene as a continuous film, using the interfacial polymerization technique. The ready availability of such films stimulated many investigations of the interesting properties of the material. The morphology of the polymer depends on the preparation conditions; films have been reported to be either fibrillar[2,3] or lamellar[4]. The properties of polyacetylene prepared by direct routes have been reviewed[5–7]. More recent syntheses allow preparation of polyacetylene from precursor polymers. Films of such precursor polymers can be spin-coated or cast onto substrates to give, after thermal conversion, fully dense polyacetylene coatings or free-standing films. Oriented films may be obtained by stretch alignment of the precursor during thermal conversion. We describe here an investigation of the structural parameters, the state of order and the photophysical properties of polyacetylene prepared from precursor polymers with different chemical structures and molecular weight distributions, and we compare the results with those of earlier work. We find that the structural properties of precursor-route polyacetylene depend strongly on several factors, including the conversion protocol adopted, the chemical structure and microstructure of the precursor, and the molecular weight distribution. These factors also affect the photophysical properties of polyacetylene, as assessed from optical absorption and photoinduced absorption. From this comparative study of structural and photophysical properties of polyacetylene we conclude that various types of defects introduced during synthesis have specific influences on the state of order and the stabilization of photogenerated excitations in this polymer.

Information has been published on the unit cell *cis*-polyacetylene[4,8,9], *trans*-polyacetylene[10–15] and on the evolution of the structure during the isomerization process[15–17]. Both the lateral arrangement and the chain repeat unit are different for the two forms of the polymer[16–18]. The difference in the lateral packing is small, however, which allows both isomerization states to be present in the same crystallites. This conclusion is supported by the observation of a continuous change in the lateral spacings during isomerization[16,17], which also indicates that the crystallinity is retained.

Polyacetylene can be prepared via various precursor polymer routes[19,20]. The original route, which we term here the 'standard Durham route'[19] allows conversion of the precursor into the final polymer in the solid state. As-cast films of standard Durham precursor thermally transformed to *trans*-polyacetylene are found to show very small crystallites[21–23], typically 45 Å. For oriented materials, higher crystallite size and degree of crystallinity are usually observed[13,21,23]. This suggests that orientation, either by alignment in fibres or stretching, is essential for crystallization, and consequently the atomic arrangement in the crystallites may not be the thermodynamic equilibrium structure. This may explain the discrepancies in structures found in the literature, which we suggest may depend on the preparation history of the material. In spite of the disagreement on the space group, the consistency in the

* To whom correspondence should be addressed

0032-3861/94/020403-12
© 1994 Butterworth-Heinemann Ltd.

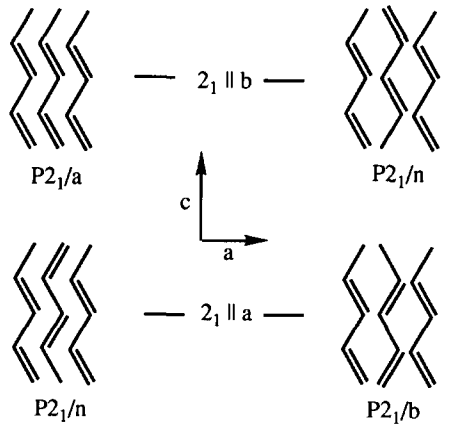

Figure 1 Possible space groups of dimerized *trans*-polyacetylene compatible with the projected space group p2gg

fundamental unit cell parameters makes structural investigations, especially comparisons of disorder, a useful exercise.

trans-Polyacetylene has a chain repeat length variously reported[10–14] in the range 2.26–2.47 Å. Bond length alternation, modelled to arise from Peierls distortion[24,25], is about 5%. The dihedral angle between adjacent carbon–carbon bonds can be calculated from the average bond length and the repeat length to be 123°. Chemical and electronic defects, such as remaining *cis*-units from the isomerization, sp^3 defects, and bond-order defects (solitons), can affect the chain repeat length. The chain is elliptical in cross-section, with a ratio of major to minor axes of 1.3:1. This nearly circular cross-section is important when considering the packing of chains. The two-dimensional space group is reported as p2gg. *Figure 1* shows the different possible structures based on p2gg, assuming dimerization of the chains, i.e. bond length alternation. Neglecting dimerization, the space groups $P2_1/n$ ($2_1 \parallel b$) and $P2_1/b$ become Pbnm, and $P2_1/a$ and $P2_1/n$($2_1 \parallel a$) become Pnam. Many reports suggest a structure that is close to pseudo-hexagonal packing, which is the optimal packing of circular cross-section entities. This arrangement fixes a relationship of the crystallographic parameters of $a^2 = 3b^2$.

Pseudo-hexagonal packing results in the coincidence of a number of reflections. Determination of a structure close to pseudo-hexagonal is hampered by the difficulty of distinguishing these close reflections due to peak broadening. Two reports[18,23] suggest a slight splitting of the 1 1 0 and 2 0 0 reflection. Another problem arises from the interpretation of the 0 0 l, $l \neq 2n$ reflections. These reflections are only allowed if the bond alternation is in phase ($P2_1/a$ and $P2_1/b$: see *Figure 1*). The intensity of the 0 0 1 reflection was therefore used to estimate the amount of bond alternation. However, other structural properties can influence the intensity of this reflection, which casts doubt on the use of the 0 0 1 reflection for this interpretation. Thus, there is considerable disagreement in the literature on the space group of polyacetylene: *Table 1* summarizes some of the structures suggested previously.

As indicated above, the state of order/disorder in polyacetylene prepared from precursor routes can be varied over a wide range, first by using different precursor polymers and secondly by varying the processing of these precursors (e.g. spin-coating on substrates to give highly disordered films or stretch alignment to form free-standing crystalline samples). It is widely recognized that the morphology in samples of conjugated polymers directly influences the degree of conformational order, i.e. the extent of unperturbed planar conjugated chain segments.

The band-gap, as seen in optical absorption, is a direct measure of the extent of conjugation and the presence of conjugation-breaking or weakening defects (chain bends, chain twists/rotations, sp^3 and other chemical defects, interchain coupling, etc.). Thus, we can attempt to relate structural parameters of polyacetylene prepared via various routes to processes that influence the electronic structure/conjugation. Also, much of the interest in conjugated polymers is due to the presence of strong non-linear interactions, e.g. the possibility of photoproducing excitations that form new states within the band-gap (solitons, polarons, bipolarons)[26]. It has already been shown, to some extent, that the stability of such excitations depends strongly on the morphology of the material and the presence of defects that act as pinning sites for excited states[27–33]. It is a further aim of this paper to compare the morphology of the forms of polyacetylene investigated with the measurements of quasi-steady-state photoinduced absorption, which gives information on the behaviour of photoexcited metastable band-gap states.

EXPERIMENTAL

The original version of the Durham precursor route is shown in *Figure 2* (route A–B–C–*trans*-polyacetylene). The double bonds in the backbone of polymer B may have *cis* or *trans* stereochemistry. The frequency and distribution of such units depends on the experimental details of the polymerization of A to B, the nature of the propagating chain end being the main determining factor. The solvent concentration also influences the outcome. The double bonds in B are not spontaneously isomerized and their distribution and frequency have an effect on properties of B, such as its conformational mobility and solubility. These factors influence the detailed nature of precursor films and their subsequent conversion to polyacetylene. The conversion is a complex process involving the elimination of hexafluoroxylene from the backbone of precursor polymer B, the migration and loss of this eliminated molecule from the film and the isomerization of the nascent polyene sequences to *trans*-polyacetylene. The isomerization is catalysed by

Table 1 Reported structures of *trans*-polyacetylene

Ref.	Material[a]	*a* (Å)	*b* (Å)	*c* (Å)	α (degree)	Space group
10	SPA	7.32	4.24	2.46	90	Pnam
12	SPA	4.24	7.32	2.46	91.5	$P2_1/n$
16	SPA	7.41	4.08	2.26	90	–
9	SPA	7.41	4.08	2.46		$P2_1/a$
17	SPA	7.38	4.09	2.46	–	–
11	sDPA	7.20	4.15	2.44	90	–
14	sDPA	4.18	7.34	2.42	90.5	–
13	sDPA	7.35	4.24	2.47	87–93	$P2_1/b$ or $P2_1/n$
This work	iDPA	7.25	4.19	2.43	90	Pnam

[a] SPA, Shirakawa polyacetylene; sDPA, standard Durham polyacetylene; iDPA, improved Durham polyacetylene

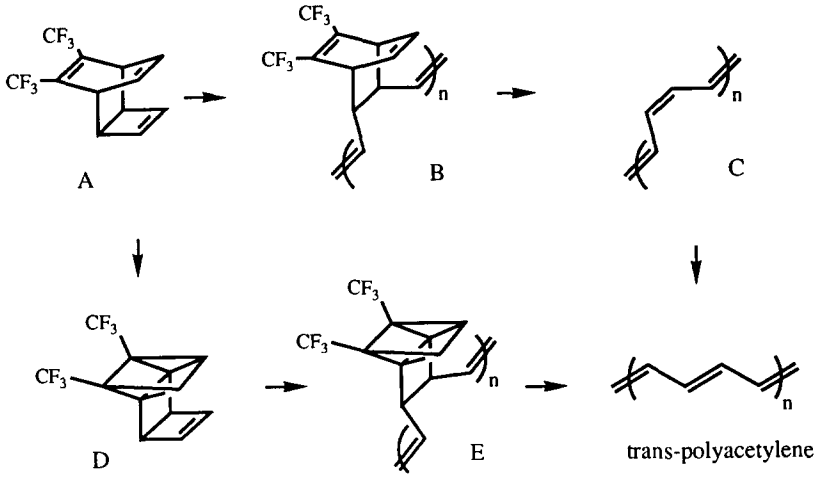

Figure 2 Synthetic routes to Durham polyacetylene

trace impurities such as dioxygen, and proceeds readily as the polyene chain length increases. These processes overlap in time and space and the detailed structure of the polyacetylene films produced by this route is dependent on the preparation protocol adopted as well as the nature of the precursor B.

In most of our earlier work on Durham polyacetylene we have used material prepared with an initiator derived from the reaction of tungsten hexachloride and tetramethyl tin; the exact nature of the initiator (or initiators) resulting from this reaction is not known but the precursor polymer B has roughly equal amounts of *cis*- and *trans*-vinylenes, which are thought to be statistically distributed. The polymer has a relatively broad molecular weight distribution. If a well-defined initiator of the kind introduced by Shrock is used, namely Mo(=CH–t-Bu)(NAr)(O–t-Bu)$_2$, then living polymerization results and the molecular weight distribution of the product precursor polymer is narrow, and controlled simply by the ratio of monomer to initiator. We term the polymer made via this route 'improved Durham polyacetylene'. In *Table 2* are listed the calculated and observed number average molecular weight values ($\bar{M}_n$) for the different precursors to improved Durham polyacetylene prepared for this work.

The precursor polymer undergoes a slow conversion to polyene, even at 0°C, and consequently it is difficult to produce totally reliable molecular weight distribution data. Since g.p.c. columns are expensive we were loath to carry out many analyses. The calculated $\bar{M}_n$ values are derived from the molar ratio of initiator to monomer on the assumptions of 100% monomer conversion and a polymer chain initiated by each initiator molecule. The corrected experimental $\bar{M}_n$ values listed in *Table 2* indicate that these assumptions are valid within the errors of measurement. It should be noted that samples S4 and S5 appeared to be bimodal on g.p.c. analysis, with weak peaks at very high masses (20 and five times the expected values, respectively); we attribute this to polymer aggregation in solution in these samples but, for the reasons indicated above, were unwilling to risk our g.p.c. column in an extensive investigation of this phenomenon.

Another consequence of using this particular initiator is that the overwhelming majority of the vinylenes in the backbone of the precursor B (*Figure 2*) are *trans*[34]. This improvement in the precision and control with which the

Table 2 Precursor samples of improved Durham route polyacetylene. Experimental g.p.c. values against polystyrene standard

Sample	$\bar{M}_n$ Calculated	$\bar{M}_n$ Experimental[a]	$\bar{M}_w/\bar{M}_n$
S1	42 120	45 880	1.25
S2	61 320	67 280	1.33
S3	74 935	–	–
S4	21 519	[b]	–
S5	75 000	[b]	–
S6	174 880	149 000	1.3
S7	33 700	–	–
S8	286 100	268 800	1.46

[a] G.p.c. in tetrahydrofuran, PLgel column, 10 μm, 10^4 Å, 0°C, corrected using data from ref. 65

[b] Samples appeared to be bimodal with peaks at high mass possibly due to aggregation in solution

synthesis of B may be carried out is anticipated to have an effect on the control of precursor film formation and the detailed structure of the final product, *trans*-polyacetylene. In particular, the capacity to make batches with narrow molecular weight distributions and well-defined molecular weights allows the formulation of any required molecular weight distribution. This is likely to be of considerable importance, since it is well established that properties of films, such as flow and cohesive strength, are a function of molecular weight distribution. It is also expected that stretch-alignment processes are influenced by the given molecular weight distribution.

Figure 2 also shows a modified precursor route to polyacetylene (A–D–E–*trans*-polyacetylene). The precursor E has improved thermal stability over B. The properties of polyacetylene prepared from this photoisomer precursor are discussed in more detail elsewhere[20,35,36].

For our structural work we have prepared samples of improved Durham polyacetylene from a bimodal sample of precursor polymer B prepared by mixing 110 mg of sample S6 and 50 mg of sample S7 in 10 ml 2-butanone (see *Table 2*). It was observed that films from this bimodal sample could be stretched easily, whereas the monomodal samples S6 or S8 could only be stretched to very small draw ratios ($l/l_0 < 2$). It is not yet well understood why the difference in the ability for stretch alignment between mono- and bimodal samples is so pronounced.

Stretching of films of the improved Durham precursor

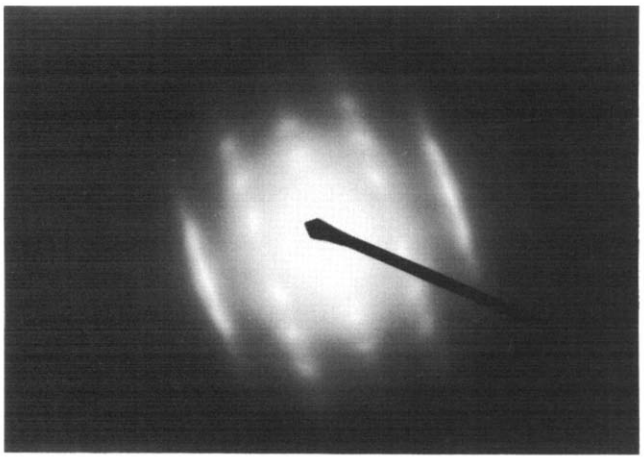

Figure 3 Electron diffraction pattern of stretch-aligned improved Durham polyacetylene ($L/L_0 = 10$)

was carried out under dynamic vacuum ($p < 10^{-4}$ mbar) at elevated temperatures. At temperatures of ~ 70°C the films could be drawn readily within short time-scales ($t < 5$ min). We believe that the drawing and conversion processes overlap in time and space due to plasticization of the transforming polymer by the eliminated hexafluoroxylene. Full conversion and isomerization of the materials was carried out in the stretching apparatus at temperatures of ~ 110°C for $t > 18$ h.

Room temperature transmission electron microscopy (TEM) was carried out using a Jeol 2000EX, operating at 200 kV. The images were recorded on Agfa Scientia film. Polyacetylene films stretched to high draw ratios were sufficiently thin to be used for TEM without further processing.

For X-ray studies, a Stoe diffractometer was used in transmission geometry. For the measurement of molecular orientation, single pieces of stretched materials were used. Due to the small scattering power of single-layer samples, only the strongest equatorial reflection (1 1 0/2 0 0) could be detected, and rocking curves for the assessment of the orientation were recorded from these reflections.

The peak widths were corrected for instrumental broadening according to

$$FWHM^2 = \beta^2 + I^2$$

where β is the measured and $FWHM$ the corrected peak width, and I is the instrumental broadening, which was estimated to be 0.5°. To evaluate peak broadening, Gaussian functions were usually fitted to the observed data after subtraction of the background scattering. Rocking curves were measured over a χ-range sufficiently large to ensure that the background was measured on both sides of the peak. Fits were carried out using the central 80% of the peak data, since statistical errors of the count rates are strongest at the tails of the peaks, thus leading to inaccurate fits.

For measurements of the equatorial scattering profile, several pieces of film were stacked on top of each other to increase the scattering power of the sample. The segments were glued together at the ends to avoid glue in the scattering area. To ensure that the orientations of the individual segments matched, the stacking was carried out under a microscope. For the analysis of the peak widths the measured profiles were corrected as described above.

For optical experiments the precursor polymers were spin-coated on spectrosil substrates and then converted to polyacetylene under high vacuum. Optical densities of the films, measured as $\log(T_0/T)$ in a Perkin–Elmer λ-9 u.v.–vis.–n.i.r. spectrophotometer, were usually between 0.7 and 1.2. All experiments and sample handling were carried out in an inert atmosphere or high vacuum. Quasi-steady-state photoinduced absorption was measured in a standard pump/probe set-up, with the sample in a He-flow cryostat, and a wide range of pump intensities, temperatures and chop frequencies was used. For all the spectra on photoinduced absorption, which are shown below, the experimental conditions were as follows: temperature ~ 20 K, chop frequency 14, 19 or 37 Hz, pump energy 2.4 or 2.7 eV, pump intensity ~ 100 mW cm^{-2}.

STRUCTURE OF UNORIENTED AND STRETCH-ALIGNED IMPROVED DURHAM POLYACETYLENE

Crystal structure of improved Durham polyacetylene

A typical electron diffraction pattern is shown in *Figure 3*, and clearly shows fibre symmetry. Reflections are recorded up to the fourth layer line, with distinct reflections up to the second layer line. From the meridional reflection on the fourth layer line the intrachain repeat distance can be measured to be 2.45 Å. This is in good agreement with previously reported structures (Durham and Shirakawa polyacetylene)[10–14,16,17]. Five reflections on the equator are visible. The spacings of the equatorial reflections and layer line reflections are given in *Table 3*.

Based on all reflections, we have refined the structural model in an orthorhombic unit cell. The resulting indices of the reflections are also given in *Table 3*. The lattice parameters after refinement are: $a = 7.25 \pm 0.01$ Å; $b = 4.19 \pm 0.01$ Å; $c = 2.43 \pm 0.01$ Å.

Table 3 Reflection positions on electron diffraction pattern of stretch-oriented improved Durham polyacetylene

	$d_{observed}$ (Å)	Index	$d_{calculated}$[a] (Å)
Equator	3.61 ± 0.05	2 0 0	3.63
		1 1 0	3.63
	2.78 ± 0.05	2 1 0	2.74
	2.09 ± 0.05	0 2 0	2.09
		3 1 0	2.09
	1.82 ± 0.05	4 0 0	1.81
		2 2 0	1.81
	1.36 ± 0.05	4 2 0	1.37
		5 1 0	1.37
		1 3 0	1.37
	1.24 ± 0.05	6 0 0	1.21
		3 3 0	1.21
		5 2 0	1.21
First layer line	2.10 ± 0.05	0 1 1	2.10
	1.55 ± 0.05	1 2 1	1.55
	1.13 ± 0.05	2 3 1	1.15
	1.18 ± 0.05	4 2 1	1.19
		5 1 1	1.19
		1 3 1	1.19
Second layer line	1.22 ± 0.05	0 0 2	1.22
	1.16 ± 0.05	2 0 2	1.15
		1 1 2	1.15
	1.05 ± 0.05	0 2 2	1.05
		3 1 2	1.05

[a] Calculated spacings based on the orthohombic unit cell

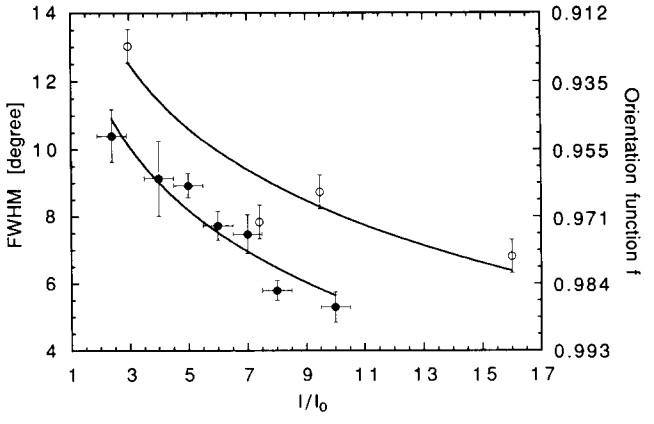

Figure 4 Radial *FWHM* of 1 1 0/2 0 0 reflection *versus* draw ratio for single films of standard (○) and improved (●) Durham polyacetylene (data for standard Durham polyacetylene from refs 13, 37)

It should be mentioned that the reflections at 1.13 and 1.18 Å on the first layer line are very close, and are difficult to distinguish. It is possible that they are indicative of a slight deviation from an orthorhombic unit cell into a monoclinic cell. These reflections should then be indexed $h\,k\,l$ and $h\,\bar{k}\,l$. We therefore attempted to fit a monoclinic unit cell to all reflections, but found that resulting unit cell parameters deviate only slightly from those for the orthorhombic unit cell, and depend on which index is given to the split reflections. Within the accuracy of our data, it was therefore not possible to choose one monoclinic cell unambiguously.

Orientation of stretched films

The molecular orientation of stretched films of improved Durham polyacetylene with different draw ratios was determined by measuring the arcing of the strong equatorial reflection (1 1 0/2 0 0) with diffractometer scans. The result is shown, together with results of similar measurements on standard Durham polyacetylene[13,37], in *Figure 4*. The orientation is presented in terms of the *FWHM* of the corrected rocking curves, and the Hermans orientation function, *f*,[38,39]:

$$f=\frac{3\cos^2\langle\Phi\rangle-1}{2}$$

where the average azimuthal angle, $\langle\Phi\rangle$, is taken to be the *FWHM* of the intensity distribution of the reflection.

The error of the *FWHM* reflects the fluctuation of these values if the fit was carried out to 60–100% of the peak data. In a full analysis of the orientation it would be necessary to obtain the orientation function of the crystallites by deconvolution of the intensity. An example of this analysis in the context of liquid crystals is reported by Deutsch[40]. Because we are only concerned with the change of orientation with increasing stretch ratio, the above treatment is sufficient and is usually followed.

We see that increased stretching of the material results in enhancement of the molecular orientation. The highest orientation function obtained, for a sample with a draw ratio of 10, was 0.987 ± 0.003, which is considerably higher than those obtained for standard Durham polyacetylene and other conjugated polymers, such as poly(*p*-phenylene vinylene) (PPV)[41,42]. Our results show that stretching of improved Durham polyacetylene results in higher orientations for the same draw ratio over the entire range of stretching ratios, and that for a lower stretch ratio a higher final orientation can be achieved. Even for stretch ratios as high as 10 and 16, for improved Durham polyacetylene and standard Durham polyacetylene, respectively, the orientation functions have not reached convergence. This is in contrast to measurements on PPV, where convergence is reached for a stretch ratio of six[42]. We note that stretching in polyacetylene is essential for crystallization, whereas it is not in PPV. This can clarify the behaviour, to some extent, as it suggests that in PPV stretching results in alignment of crystalline regions, whereas in Durham polyacetylene individual chains have to be aligned, and it can only crystallize after some degree of alignment has been achieved. Comparison of data for polyacetylene and PPV may indicate, therefore, that the mechanism leading to oriented samples is different for the two polymers.

Although our data do not give conclusive evidence that the highest possible orientation has been achieved for either polyacetylene, they suggest that improved Durham polyacetylene can be oriented to a higher extent than standard Durham polyacetylene. It is not yet clear to us whether this is due to the more stereoregular precursor or to the different molecular weight distribution in our improved Durham polyacetylene.

Equatorial scans of the same single-layer samples were also recorded. Due to the small sample thickness, only the strong 1 1 0/2 0 0 reflection could be observed. We have attempted to follow the changes of the peak maximum and the broadening of the reflection. However, neither of these parameters showed a clear trend with changing stretch ratio. We believe the reason for this can be found partly in a variation of thickness of the different samples, as can be seen from strong variations in the overall scattering power of the samples. It should be mentioned that for standard Durham polyacetylene[37] also, no clear dependence of the peak broadening on the stretch ratio could be established.

Crystallite size and disorder

A summary of possible forms of disorder that can affect the diffraction patterns of polyacetylene was reported by Bott *et al.*[15]. In our analysis we focus primarily on an interpretation within a paracrystalline lattice model[43].

Figure 5 shows a diffractometer scan of a 10-layer film of unstretched improved Durham polyacetylene. Conversion and isomerization were carried out at 120°C.

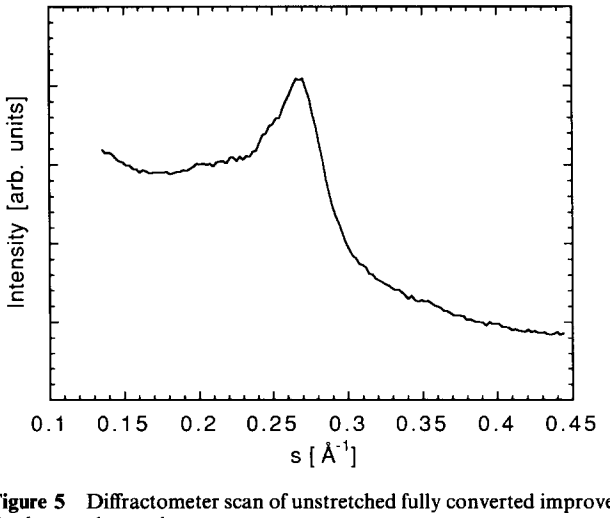

Figure 5 Diffractometer scan of unstretched fully converted improved Durham polyacetylene

The data show some splitting of the main peak, indicative of a deviation from pseudo-hexagonal packing. As only one diffraction peak can be observed, only a simple model can be applied and the crystallite size, L, can be determined by the Scherrer formula[44]:

$$L=\frac{k\lambda}{\beta_0 \cos \vartheta}$$

where β_0 is the $FWHM$ of the reflection at a Bragg angle of ϑ; λ is the X-ray wavelength; and k is the Scherrer parameter, taken as 1.

After subtraction of the background it becomes apparent that the main peak ($s \approx 0.27$ Å^{-1}) shows a shoulder towards lower scattering angles ($s \approx 0.21$ Å^{-1}). This suggests that the feature is a superposition of two peaks, and therefore two superimposed Gaussian functions have been fitted to the data. The observed broadening corresponds to a crystallite size of 35 ± 5 Å. This value is derived from the stronger peak, as the fit for this one can be regarded as more accurate. For standard Durham polyacetylene the diffraction pattern is very similar and the crystallite size is reported[15,23] to be dependent on the isomerization temperature. The crystallite size we obtain for improved Durham polyacetylene is less than the value reported for standard Durham polyacetylene (~45 Å)[15,23]. The crystallite size in unoriented Shirakawa polyacetylene is usually larger than this, ranging from 63 Å (ref. 45) to 93 Å (ref. 46). This is presumably due to the usually fibrillar structure of Shirakawa polyacetylene, in which the fibrils can be regarded as crystallites. This results in polycrystalline films in the Shirakawa polymerization.

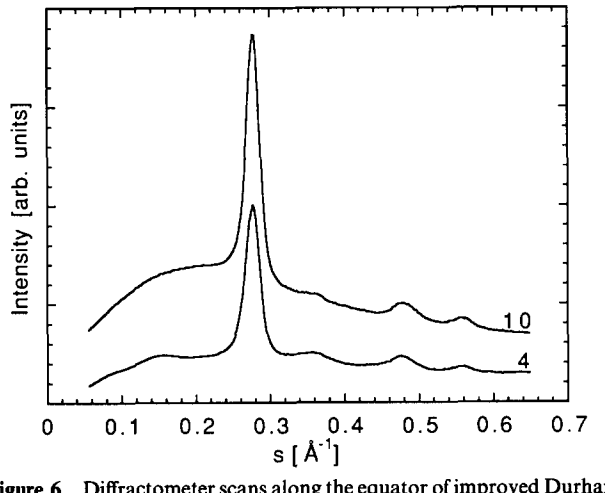

Figure 6 Diffractometer scans along the equator of improved Durham polyacetylene with stretch ratios of 4 and 10 (intensities are corrected with Lorenz and polarization factors; the scans are normalized for $2\vartheta = 60°$ and displaced)

For stretched materials, diffractometer scans showed more reflections, and therefore a more advanced model can be applied. Based on a paracrystalline lattice model[43] we analysed the peak broadenings of the reflections in a full equatorial scan of a multilayer film of stretched material. This model describes the structure in terms of nearest-neighbour distances instead of an ideal periodic lattice. The materials that are appropriately described by it stand between an amorphous structure and an ideal crystal. To describe the state of order in the material, two kinds of disorder are used: disorder of the first kind refers to statistical or thermal deviation of the atoms from the ideal lattice position; disorder of the second kind is the mean square displacement of the distance, d, between two nearest-neighbour lattice points. In the diffraction patterns, disorder of the second kind is observed on decrease of intensity and increase in reflection broadening with increasing scattering vector, s. This broadening is additional to a constant broadening arising from finite crystallite size. By assuming that the disorder of the second kind and the crystallite size, L, can be described by Gaussians with $FWHM$ of $(\pi^2\Delta^2/d)s^2$ and $1/L$, respectively, the $FWHM$ of the reflections is given by:

$$FWHM^2=\frac{1}{L^2}+\frac{\pi^4\Delta^4 s^4}{d^2}$$

The samples used were stretched and several pieces from one film were stacked on top of each other. Scans taken from two samples with stretch ratios of 4 and 10, and with 12 and 15 stacked layers, respectively, are shown in *Figure 6*. Measurements on samples with different stretch ratios were carried out to investigate further the dependence of line broadening on the draw ratios; the quantitative results are shown in *Table 4*.

The sample with lower stretch ratio exhibits intensity maxima with a better peak-to-background ratio. This can be interpreted by considering the sample thicknesses. Drawing of the material to a higher extent results in thinner films, as very similar thicknesses and sizes of precursor films were used for each individual sample; for multilayer samples with a compatible number of layers, the overall sample thickness therefore decreases with increasing draw ratio.

Comparison of the data for unstretched and stretched material shows that splitting of the main peak is only observed for unstretched polyacetylene. For the stretched material, peak widths are usually narrower, and thus splitting should be more noticeable. This behaviour suggests that stretching of polyacetylene results in an alteration of the packing of the chains. This observation supports the previously stated hypothesis that, due to

Table 4 Peak positions and widths of stretched improved Durham polyacetylene

	$I/I_0 = 4$		$I/I_0 = 10$	
Index	s (Å^{-1})	$FWHM$ (Å^{-1})	s (Å^{-1})	$FWHM$ (Å^{-1})
110/200	0.276±0.005	0.0218±0.0005	0.277±0.005	0.0186±0.0005
210	0.360±0.005	0.0354±0.0005	(0.36)[a]	-
020/310	0.477±0.005	0.0349±0.0005	0.481±0.005	0.0321±0.0005
220/400	0.557±0.005	0.0240±0.0005	0.560±0.005	0.0251±0.0005

[a] Very low accuracy

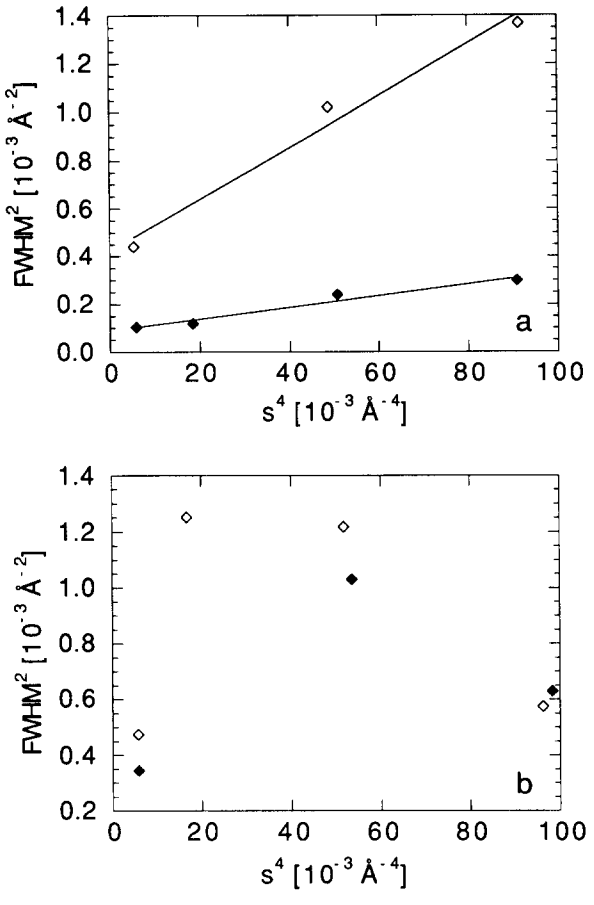

Figure 7 *FWHM*^{2} *versus* s^4 for polyacetylene prepared by different routes and drawn to different stretch ratios. (a) Standard Durham polyacetylene (◇) from ref. 37, and Shirakawa polyacetylene (◆) from ref. 18. (b) Two samples of improved Durham polyacetylene

strain, the packing in stretched material may not be the one that is favoured thermodynamically.

The broadening of the intensity maxima was analysed by a Gaussian fit to the peaks, with the background subtracted. The corrected broadenings are summarized in *Table 4*. The peak positions quoted in the table are the centres of the fitted Gaussian functions and not the observed maxima, which showed small deviation from this position. All positions are in good agreement with those found in the electron diffraction pattern (see *Table 3*). However, the statistical quality does not provide sufficient accuracy to compare peak positions of the samples with different draw ratios. The influence of statistical fluctuations on the peak widths, however, was much smaller, and we derive an error of approximately 5×10^{-4} Å^{-1} for these values.

Plotting s^4 against the *FWHM*^{2} allows us to distinguish graphically between peak broadening from finite crystallite size and disorder of the second kind. This is shown in *Figure 7*, together with data published for standard Durham polyacetylene and Shirakawa polyacetylene for comparison.

Although peak broadening in standard Durham polyacetylene and Shirakawa polyacetylene can be adequately described by application of a one-dimensional paracrystalline lattice model, it becomes obvious from *Figure 7* that this is not possible for improved Durham polyacetylene. The one-dimensional model successfully used by Sokolowski *et al.*[13] implies that the disorder and crystallite size is isotropic in all directions. This isotropic behaviour would be expected if the molecules in the two-dimensional projection were circular entities. However, as mentioned earlier, they are elliptical with a ratio of major to minor axes of 1.3:1. Thus a two-dimensional description would seem more appropriate. A two- or three-dimensional paracrystalline lattice model establishes the linear dependence of *FWHM*^{2} on s^4 only for peaks of the same reflection family, i.e. $(h,k,0)$–$(2h,2k,0)$–$(3h,3k,0)$–.... The only peaks fulfilling this condition are the first and last, i.e. the 1 1 0/2 0 0 and 2 2 0/4 0 0 reflections. It is clear that a one-dimensional paracrystalline lattice does not hold for improved Durham polyacetylene; it is expected that the crystallite size and disorder in the 1 1 0 direction will be different from those in the 1 0 0 direction. Determination of the crystallite size and disorder in these directions therefore requires a deconvolution of the peaks. This is only possible if the relative intensities of the overlapping reflections are known. These intensities depend on the setting angles. Values from 24 to 60° have been reported[10,13], a range too wide to allow approximation of the ratio of the two intensities. The peak broadening of the composite peak will be determined by the stronger peak or, if they are of compatible intensity, by the broader peak. If one of the reflections is predominant the crystallite size and disorder will represent the values for this reflection, and if they are of similar intensity they will represent limiting values (lower limit for crystallite size, upper limit for disorder) for the paracrystalline parameters. The values are: $L = 46$ Å, $\Delta = 0.12$ Å, for $L/L_0 = 4$; $L = 55$ Å, $\Delta = 0.15$ Å, for $L/L_0 = 10$.

The difference in the parameters for the two stretch ratios is small, and the parameters can be regarded as characteristic for the material. This allows a comparison to be made with polyacetylene prepared by other routes. The crystallite size is of the same order as values published for standard Durham polyacetylene[13]; the disorder obtained for improved Durham polyacetylene is considerably smaller than for standard Durham polyacetylene[13]. Comparison with data from Shirakawa polyacetylene ($L = 100$ Å and $\Delta = 0.14$ Å) shows that the improved Durham polyacetylene shows a lower crystallite size.

The crystallite size along the chain direction was determined from the peak broadening of the 0 0 2 reflection with the Scherrer formula, and was found to be 70 Å. This is in rough agreement with values reported for standard Durham polyacetylene (80 Å)[37].

Structural changes with oxidation

Polyacetylene is very susceptible to oxidation, and this is known to have a strong effect on the properties of the material (oxygen doping or carbonyl formation)[47]. We have attempted to follow some structural changes arising from the oxidation process: equatorial diffractometer scans were recorded after different times of air exposure to the multilayer sample with a stretch ratio of 4. The first experiment ($t = 0$ days) was started a few minutes after removal of the sample from an inert gas atmosphere. The data are shown in *Figure 8*. The scan parameters were set to a step width of 0.2° over a range of 5–110° and 5 min per step. Consequently, about 8 h passed from the beginning of the scan to the maximum of the 1 1 0/2 0 0 reflection.

It should be mentioned that the air exposure might have affected the scan at $t = 0$ days, as 8 h passed before

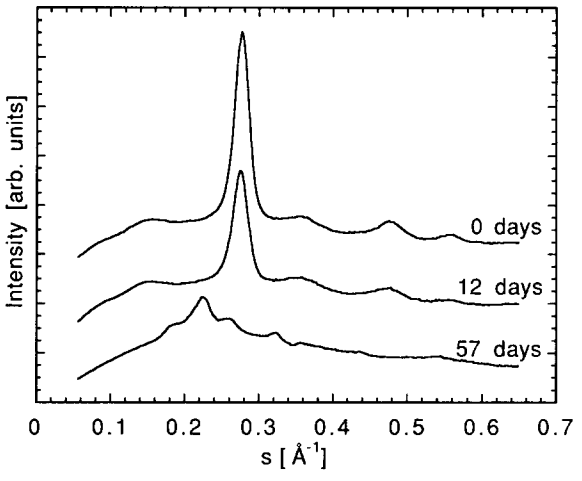

Figure 8 Diffractometer scans along the equator of improved Durham polyacetylene after different stages of air exposure (time of exposure is given in the diagram; intensities are corrected with Lorenz and polarization factors; the scans are normalized for $2\vartheta = 60°$ and displaced)

Table 5 Broadening of the equatorial reflections at different stages of exposure to air

	Broadening ($Å^{-1}$)		
Index	$t = 0$ days	$t = 12$ days	$t = 57$ days
110/200	0.0218	0.0150	0.0131
210	0.0354	0.0261	0.0095
020/310	0.0349	0.0239	0.0095
220/400	0.0240	0.0170	0.0352

the first peak was measured, and Brown *et al.*[23] have reported on intensity decreases in standard Durham polyacetylene during the first hours of exposure to air. The most noticeable effect during early stages of the oxidation ($t = 12$ days) is an overall decrease of the peak intensity. This reduces the ratio of peak intensity over background intensity and can be interpreted as a reduction in crystallinity. No significant shifts of the four observed peaks can be noticed. Most of the peaks become significantly sharper, as can be seen from *Table 5*.

After short times the amount of oxygen in the material can be assumed to be low, as large amounts are expected to noticeably widen the lattice. Such a widening of the lattice, which would be observed by shifts of reflections towards lower angles, is not found by a comparison of the scans for $t = 0$ days and $t = 12$ days.

After longer exposure to air ($t = 57$ days) the peak-to-background ratio has decreased further, indicating very low crystallinity. Additionally, a shift of all peaks to lower angles is observed, indicating a widening of the lattice due to the inclusion of oxygen. The positions of the main features are 4.48, 3.86 and 3.12 Å. Again, a sharpening of the peaks can be observed. The broadening of the main peaks are listed in *Table 5*. As the peaks have shifted, it is not immediately clear whether the indexing used for pristine polyacetylene is applicable to the oxidized material. However, it is reasonable to assume that the low-angle reflections in pristine polyacetylene will become the low-angle reflections of the oxidized material. The composite peak (1 1 0/2 0 0) in pristine polyacetylene is then found to split, as there is a deviation from the pseudo-hexagonal structure. It is possible to obtain a good fit to the peak positions if the first reflection (4.48 Å) is indexed 1 1 0 and the next (3.86 Å) as 2 0 0. The next feature of the profile at 3.12 Å can then be identified as the 2 1 0 reflection. This allows us to establish the unit cell of the oxidized material: $a = 7.72$ Å, $b_\perp = 5.50$ Å.

On the basis of our results we propose the following model of oxidation[47]. Oxidation occurs in the first instance in less ordered regions of the film, possibly because there is a less dense packing of the polyacetylene matrix structure and hence more, and wider, diffusion channels are available. It was reported that unoriented standard Durham polyacetylene oxidizes more rapidly than the more crystalline Shirakawa material[47]. The ordering of these regions is consequently further decreased, and their crystalline character is lost. The scattering from these regions is therefore observed as background and not as discrete Bragg reflections. The scattering we observe in discrete maxima arises from pristine polyacetylene regions, which are, as mentioned earlier, of higher order than the average in the original film. The disorder derived from peak broadening is hence reduced. After further oxidation, a structure forms that includes oxygen between the polyacetylene chain, as indicated by the shift in the peak position. We note that oxygen uptake in standard Durham polyacetylene is considerable[47], ~2 wt% in the first 5 min at 80°C. The overall crystallinity of the material reduces during the entire oxidation process. It should be noted that this model suggests that highly disordered spin-coated films of polyacetylene are more likely to be affected by (unintentional) doping.

Comparison of our results with data obtained for standard Durham polyacetylene[37,47] suggests that improved Durham polyacetylene may be more susceptible to oxidation, and significant structural changes are observed after short time-scales. However, we do not yet have sufficient data to support this observation strongly, and these differences may be due to sample variations.

OPTICAL ABSORPTION AND PHOTOINDUCED ABSORPTION OF POLYACETYLENE PREPARED BY VARIOUS PRECURSOR ROUTES

Optical absorption

Figure 9 shows the characteristic optical absorption spectra of improved Durham polyacetylene (one sample

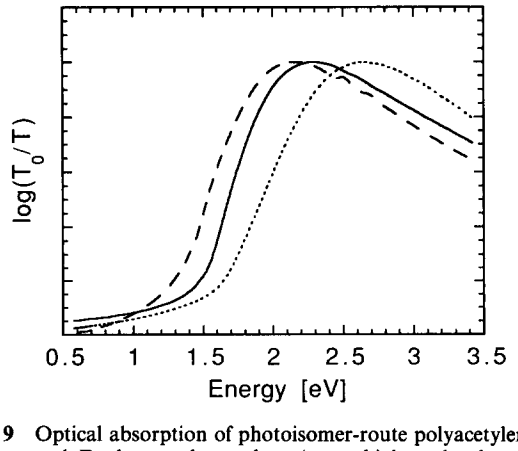

Figure 9 Optical absorption of photoisomer-route polyacetylene (····) and improved Durham polyacetylene (——, high molecular weight precursor; – – –, low molecular weight precursor). All spectra at room temperature; the optical densities are about 1; the spectra are normalized to the same peak value. The high and low molecular weight samples were prepared from samples S8 and S4 (*Table 2*), respectively

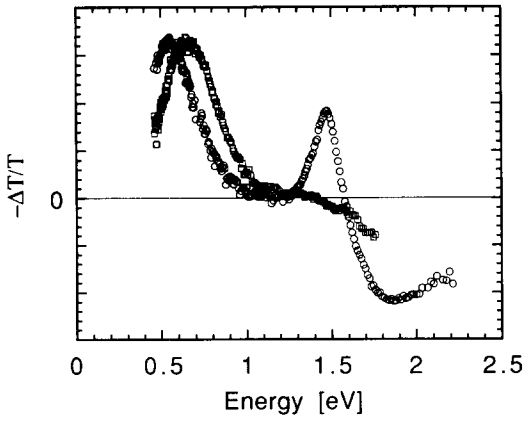

Figure 10 Photoinduced absorption of photoisomer-route polyacetylene (□) and high molecular weight precursor improved Durham polyacetylene (○, sample S8). For experimental parameters see Experimental; the spectra are normalized to the same peak value ($-\Delta T/T \approx 2 \times 10^{-4}$) and are shown on a linear scale

prepared from a high molecular weight precursor, S8 in *Table 2*, and another from a low molecular weight precursor, S4 in *Table 2*), together with a spectrum of spin-coated photoisomer-route polyacetylene (shown for comparison). The spectra show very broad absorption bands with an extended tail towards lower energies. The absorption peaks at 2.65 eV in photoisomer-route polyacetylene; the corresponding values for the improved Durham polyacetylene are typically 2.3 eV. We note that there is some sample variation in the improved Durham polyacetylene, and in samples prepared from the low molecular weight precursor the peak is as low as 2.15 eV. We have normally observed the lower peak positions in the samples prepared from the low molecular weight precursor, and this may indicate that ordering is facilitated if chains are shorter. Sample variation was found to be rather small in photoisomer-route polyacetylene. The spectra for standard Durham polyacetylene are similar[31,48] and show peak values normally around 2.5 eV. The peak position in stretched standard Durham polyacetylene[49,50] is at about 1.9 eV. Smaller values have only been observed in (polycrystalline) polyacetylene prepared by routes based on the Shirakawa synthesis. The disorder in all the precursor-route polyacetylenes smears out any vibrational structure in the absorption band. Such structured absorption has only been observed in reflection spectra of some samples of polyacetylene based on the Shirakawa route[51,52]. These spectra indicate that the intrinsic lowest lying absorption of polyacetylene[51,52] lies at about 1.5 eV.

From the structural and optical investigations presented above it can be seen that there is a correlation between the results obtained by the two methods. Crystallinity is highest, and amorphous phase content lowest, for Shirakawa polyacetylene samples, followed by stretch-oriented samples of standard and improved Durham polyacetylene, unoriented samples of standard and improved Durham polyacetylene, and finally the photoisomer-route polyacetylene[35]. In the structural investigations of unoriented Durham polyacetylene we could only observe one unambiguous reflection, which is correlated to interchain order/crystallinity. Inter- and intrachain order are related, and some evidence for this is given above in the discussion of the alignment process in polyacetylene. The conversion conditions and the interchain disorder introduced by the retained fluorine side groups in the photoisomer-route polyacetylene suppress crystallization[35]. Therefore intrachain order, i.e. the average extent of conjugation, is low and the energy gap is larger. This is consistent with X-ray analysis, which indicates a very low interchain coherence length and strong background scattering from amorphous phases. Raman spectroscopy[35] and doping experiments[53] give further evidence for the high disorder in photoisomer-route polyacetylene. The red-shift of the optical absorption of standard and improved Durham polyacetylene is consistent with this interpretation; inter- and (related) intrachain order are also higher compared to photoisomer-route polyacetylene (higher interchain coherence length).

Comparison of structural data and optical absorption between standard and improved Durham polyacetylene (unoriented films) is less unambiguous. Our structural data suggest that interchain order is higher in standard Durham polyacetylene. However, the absorption spectra of improved Durham polyacetylene are slightly red-shifted with respect to standard Durham polyacetylene. These consistently lower values in improved Durham polyacetylene may be due to the improved stereoregularity in the precursor (fewer remaining, higher energy, *cis*-linkages in the converted polymer) and/or the narrower molecular weight distributions.

Photoinduced absorption

Figure 10 shows photoinduced absorption spectra of photoisomer-route polyacetylene, shown for comparison, and improved Durham polyacetylene (high molecular weight precursor, sample S8 in *Table 2*). We have observed that the photoinduced absorption spectra of photoisomer-route polyacetylene show very little sample dependence (even for different precursor molecular weights), whereas the spectra of improved Durham polyacetylene vary more strongly (between different molecular weight precursors and within the same precursor batch). The sample variation in improved Durham polyacetylene is particularly marked for the peak near 1.5 eV. This is demonstrated in *Figure 11*, which shows photoinduced absorption spectra of two different samples prepared from the same low molecular weight precursor solution (S4 in *Table 2*), and deposited, converted and measured under the same conditions.

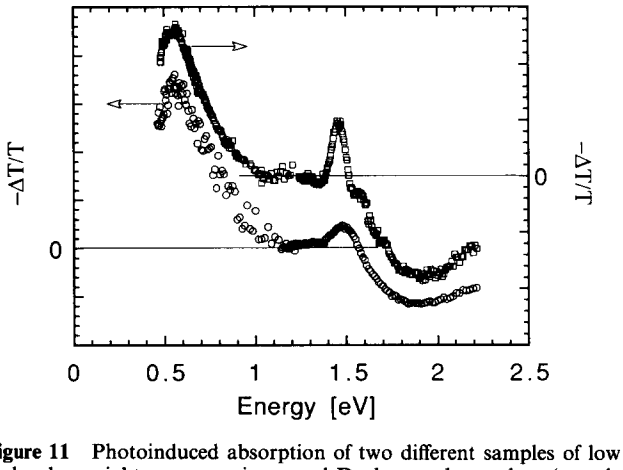

Figure 11 Photoinduced absorption of two different samples of low molecular weight precursor improved Durham polyacetylene (sample S4 in *Table 2*). For experimental parameters see Experimental; peak signal, $-\Delta T/T \approx 2 \times 10^{-4}$; linear scale

The spectra of improved Durham polyacetylene in *Figures 10* and *11* show the three characteristic features observed in photoinduced absorption in polyacetylene: near 0.5 eV the charged soliton low-energy peak, near 1.5 eV the neutral soliton high-energy peak, and above the high-energy peak bleaching of band-gap (tail) states. The position of the low-energy peak is sample dependent in improved Durham polyacetylene and lies between 0.52 and 0.55 eV (0.55 eV in unoriented standard Durham polyacetylene[31], 0.45–0.52 eV in oriented standard Durham polyacetylene[27,54,55], and 0.45 eV in Shirakawa-route polyacetylene[24,28]). The position for this peak in photoisomer-route polyacetylene is 0.65 eV (*Figure 10*). It has been shown (for Shirakawa-route polyacetylene, standard Durham polyacetylene and photoisomer-route polyacetylene) that the position of the low-energy peak scales with the energy gap[49,53]. Allowing for some sample variation, it is evident from the optical and photoinduced absorption spectra shown above that the improved Durham polyacetylene fits well into this scheme. Conformational disorder, observed in structural and optical investigations, increases the band-gap and band-gap-related photoinduced metastable states.

We note that the low-energy peak has hitherto been observed in all forms of polymer mentioned here. However, the stability of the charged soliton, which is thought to be the state responsible for the low-energy transition, is by no means exclusively determined by the intrinsic polyacetylene structure. It has been demonstrated that, at long time-scales, the low-energy signal increases with higher content of conformational defects (e.g. *cis*-content)[27,55]. A detailed comparison of the strength of the low-energy peak in various forms of polyacetylene and, for the purposes of this paper, within the series of precursor-route polyacetylenes is difficult, as a variety of experimental parameters should be exactly the same. Nevertheless, the charged soliton and hence the low-energy peak in samples of polyacetylene (disregarding the disorder of the material) seem to be intrinsic excitations, with the kinetic behaviour being affected by extrinsic factors. Theoretically, in an ideal polyacetylene crystal without disorder, the situation may be different: it has been calculated that interchain coupling in such a system would destabilize this excited state[32,56]. The negative feature observed in photoinduced absorption in figures at around 1.85–1.9 eV (onset at 1.5 eV) is simply due to bleaching of states which are moved into the band-gap. The low-energy peak and bleaching have the same temperature and chop frequency dependence and they are therefore due to the same states.

For the high-energy feature the situation is quite different; there is evidence that it is only seen if extrinsic defects are present[30]. This peak has recently been assigned to a spin 1/2 state (neutral soliton)[57]. The stability of this excitation at time-scales above microseconds (probed here) is, however, significantly more sample dependent than the charged soliton. It has been shown for standard Durham polyacetylene that the states causing the high-energy feature are localized in highly disordered regions of samples[30], and that the strength of the transition is dependent on the conversion conditions[31]. The peak scales approximately, like the low-energy peak, with the degree of conformational order and the band-gap in the sample ($\sim$1.5 eV in standard disordered Durham polyacetylene[31], $\sim$1.36 eV in Shirakawa-route polyacetylene and oriented standard Durham polyacetylene[58,59], 1.45–1.48 eV in improved Durham polyacetylene — see *Figures 10* and *11*).

The high-energy peak is absent in the highly disordered photoisomer polyacetylene (*Figure 10*). We have measured samples of standard Durham polyacetylene with absorption peaks above 2.5 eV, which is close to the 2.65 eV for photoisomer-route polyacetylene, and have observed the high-energy peak. This suggests that conformational disorder, which couples strongly to the energy gap, is not solely responsible for stabilization of the neutral soliton (see below). We believe that there are some other, yet unidentified, localized defects that stabilize the neutral soliton; the retained fluorine side groups in the photoisomer-route polyacetylene may have some effect. These issues with respect to this material are discussed in more detail elsewhere[53,60].

The various appearances of the high-energy peak in improved Durham polyacetylene (*Figures 10* and *11*) show that the position of the peak is coupled to the band-gap. The best sample with the lowest absorption peak ($\sim$2.15 eV, low molecular weight precursor) has the high-energy peak at 1.45 eV. In most of the samples of improved Durham polyacetylene (high and low molecular weight precursor) the absorption peaks at $\sim$2.3 eV and the high-energy feature at 1.47–1.48 eV. The sample variation of the neutral soliton feature compared to the charged soliton feature is more pronounced; however, we do not yet have evidence for any systematic variation. Comparison is further hampered by the possibility of different pump-intensity dependences of the two peaks.

The high-energy peak is substantially narrower for all investigated samples of improved Durham polyacetylene as compared to standard Durham polyacetylene (*FWHM* of 0.1–0.15 eV in improved Durham polyacetylene and $\sim$0.25 eV in standard Durham polyacetylene[31]). Within our series of improved Durham polyacetylene samples the peak is usually narrower in the material prepared from the low molecular weight precursor. We believe that these observations provide further support for the model of localized structural defects as the stabilizing centres for photoexcited neutral solitons, and are a reminder that the improved Durham polyacetylene precursors are much more stereoregular, possibly with a significantly reduced degree of *cis*-segments in the converted polyacetylene. We note that recent theoretical calculations indicate that photogenerated neutral solitons are not stable[61].

Interestingly, the concentration of charged defects is roughly the same (1×10^{17}–5×10^{17} cm^{-3}) for all three types and molecular weights of precursors used in this study. The values for the charge carrier concentrations were obtained from capacitance–voltage analysis of metal–insulator–semiconductor devices[53,62].

Although it is of great interest to study the photophysical properties of oriented films of polyacetylene[30,50,59], such experiments are hampered by the difficulty in preparing optically thin oriented films. For sufficient transmission in parallel polarization, films of less than 500 Å thickness are desirable, but these are very difficult to handle, and it is worthwhile to find other preparation methods. In any case, it has been mentioned above that stretch orientation of the photoisomer-route polyacetylene is generally not possible. In the case of improved Durham polyacetylene also, it has not yet been possible to obtain stretched films of the required thickness.

A promising route to prepare oriented optically thin films of polymers has been shown recently[63]. In this method, poly(tetrafluoroethylene) substrates are used to induce preferential molecular orientation in polymers[63]. We have achieved best results with the precursor-route polymer PPV, and for this material good orientation has been accomplished only if the precursor had a high content of stiff segments (e.g. conjugated units) in the backbone[64]. Preliminary attempts to apply this technique to improved Durham polyacetylene resulted in insufficient degrees of orientation, even if partially converted precursors were used, i.e. materials containing stiff *cis*- or *trans*-segments.

SUMMARY

We have compared the order in *trans*-polyacetylene films prepared via different precursor routes, and have shown that the final order has a strong dependence on the chemical and processing route. The ordering of the chains increases from photoisomer-route polyacetylene to standard Durham polyacetylene and improved Durham polyacetylene. Additionally, stretch alignment results in a more ordered system for improved Durham polyacetylene than standard Durham polyacetylene, even at lower stretch ratios. Not only can higher molecular orientation be achieved by stretch orientation in the improved Durham polyacetylene, but also the order parameters, such as disorder and crystallite size, were found to be superior for the 1 1 0/2 0 0 reflection planes of polyacetylene prepared by the new precursor route. A one-dimensional paracrystalline lattice model, as used for polyacetylene prepared by previous routes, was found to be inadequate to describe our data fully.

The positions of the optical absorption and photoinduced band-gap features are related to the state of order in the material; according to the structural improvements from photoisomer-route polyacetylene to standard and improved Durham polyacetylene, these positions shift to lower energies in the same sequence. The low-energy peak in photoinduced absorption is present in all three materials. The high-energy peak in improved Durham polyacetylene is in all cases much narrower and also usually weaker than in standard Durham polyacetylene; this is presumably due to the enhanced stereoregularity of the improved Durham polyacetylene.

ACKNOWLEDGEMENTS

We thank G. Leising and R. R. Schrock for useful discussions. We thank the Science and Engineering Research Council, British Petroleum plc and the Nuffield Foundation (R. H. F.) for financial support.

REFERENCES

1 Natta, G., Mazzanti, G. and Corradini, P. *Alti Accad. Naz. Lincei Rend. Sci. Fis. Mat. Nat.* 1958, **25**, 2
2 Ito, T., Shirakawa, H. and Ikeda, S. *J. Polym. Sci., Polym. Chem. Edn* 1974, **12**, 11
3 Karasz, F. E., Chien, J. C. W., Galkiewicz, R., Wnek, G. E., Heeger, A. J. and MacDiarmid, A. G. *Nature* 1979, **282**, 286
4 Lieser, G., Wegner, G., Müller, W. and Enkelmann, V. *Makromol. Chem. Rapid Commun.* 1980, **1**, 621
5 Chien, J. C. W. 'Polyacetylene; Chemistry, Physics, and Material Science', Academic Press, Orlando, 1984
6 Billingham, N. C. and Calvert, P. D. *Adv. Polym. Sci.* 1989, **90**, 1
7 Skotheim, T. A. (Ed.) 'Handbook of Conducting Polymers', Marcel Dekker, New York, 1986
8 Chien, J. C. W., Karasz, F. E. and Shimamura, K. *Macromolecules* 1982, **15**, 1012
9 Baughman, R. H., Hsu, S. L., Pez, G. P. and Signorelli, A. J. *J. Chem. Phys.* 1978, **68**, 5405
10 Shimamura, K., Karasz, F. E., Hirsch, J. A. and Chien, J. C. W. *Makromol. Chem. Rapid Commun.* 1981, **2**, 473
11 Lieser, G., Wegner, G., Weizenhöfer, R. and Brombacher, L. *Polym. Prepr.* 1984, **2**, 221
12 Fincher, C. R., Chen, C. E., Heeger, A. J., MacDiarmid, A. G. and Hastings, J. B. *Phys. Rev. Lett.* 1982, **48**, 100
13 Sokolowski, M. M., Marseglia, E. A. and Friend, R. H. *Polymer* 1986, **27**, 1714
14 Leising, G., Leitner, O. and Kahlert, H. *Mol. Cryst. Liq. Cryst.* 1985, **117**, 67
15 Bott, D. C., Brown, C. S., Winter, J. N. and Barker, J. *Polymer* 1987, **28**, 601
16 Robin, P., Pouget, J. P., Comès, R., Gibson, H. W. and Epstein, A. J. *Phys. Rev. B* 1983, **27**, 3928
17 Perego, G., Lugli, G., Pedretti, U. and Cernia, E. *J. Phys. Colloq. (France)* 1983, **44**, 93
18 Pouget, J. P. *Physica B* 1984, **127**, 158
19 Edwards, J. H. and Feast, W. J. *Polym. Commun.* 1980, **21**, 595
20 Feast, W. J. and Winter, J. N. *J. Chem. Soc., Chem. Commun.* 1985, 202
21 Shacklette, L. W. and Toth, J. E. *Phys. Rev. B* 1985, **32**, 5892
22 Wegner, G. *Mol. Cryst. Liq. Cryst.* 1984, **106**, 269
23 Brown, C. S., Vickers, M. E., Foot, P. J. S., Billingham, N. C. and Calvert, P. D. *Polymer* 1986, **27**, 1719
24 Su, W. P., Schrieffer, J. R. and Heeger, A. J. *Phys. Rev. B* 1980, **22**, 2099
25 Clarke, T. C., Kendrick, R. D. and Yannoni, C. S. *J. Phys.* 1983, **C3**, 369
26 Heeger, A. J., Kivelson, S., Schrieffer, J. R. and Su, W. P. *Rev. Mod. Phys.* 1988, **60**, 781
27 Pichler, K. and Leising, G. *Europhys. Lett.* 1990, **12**, 533
28 Colaneri, N. F., Friend, R. H., Schaffer, H. E. and Heeger, A. J. *Phys. Rev. B* 1988, **38**, 3960
29 Pichler, K., Halliday, D. A., Bradley, D. D. C., Burn, P. L., Friend, R. H. and Holmes, A. B. *J. Phys. Condensed Matter* 1993, **5**, 7155
30 Townsend, P. D. and Friend, R. H. *J. Phys. C: Solid State Phys.* 1987, **20**, 4221
31 Townsend, P. D. and Friend, R. H. *Phys. Rev. B* 1989, **40**, 3112
32 Vogl, P. and Campbell, D. K. *Phys. Rev. B* 1990, **41**, 12797
33 Woo, H. S., Graham, S. C., Halliday, D. A., Bradley, D. D. C., Friend, R. H., Burn, P. L. and Holmes, A. B. *Phys. Rev. B* 1992, **46**, 7379
34 Knoll, K. and Schrock, R. R. *J. Am. Chem. Soc.* 1989, **111**, 7989
35 Jones, C. A., Lawrence, R. A., Martens, J., Friend, R. H., Parker, D., Feast, W. J., Lögdlund, M. and Salaneck, W. R. *Polymer* 1991, **32**, 1200
36 Feast, W. J., Parker, D., Winter, J. N., Bott, D. C. and Walker, N. S. *Springer Ser. Solid State Sci.* 1985, **63**, 45
37 Sokolowski, M. M. CPGS Thesis, University of Cambridge, 1985
38 Hermans, P. H. and Platxek, P. *Kolloid Z.* 1939, **88**, 68
39 Hermans, J. J., Hermans, P. H., Vermaas, D. and Weidinger, A. *Rec. Trav. Chim. Pays-Bas* 1946, **65**, 427
40 Deutsch, M. *Phys. Rev. A* 1991, **44**, 8264
41 Martens, J. H. F. M.Phil Thesis, University of Cambridge, 1989
42 Gagnon, D. R., Karasz, F. E., Thomas, E. L. and Lenz, R. W. *Synth. Met.* 1987, **20**, 85
43 Hosemann, R. and Bagchi, S. N. 'Direct Analysis of Diffraction by Matter', North-Holland Publishing Company, Amsterdam, 1962
44 Scherrer, P. *Göttinger Nachrichten* 1918, **2**, 98
45 Fincher, C. R., Moses, D., Heeger, A. J. and MacDiarmid, A. G. *Synth. Met.* 1983, **6**, 243
46 Haberkorn, H., Naarman, H., Penzien, K., Schlag, J. and Simak, P. *Synth. Met.* 1982, **5**, 51
47 Billingham, N. C., Calvert, P. D., Foot, P. J. S. and Mohammad, F. *Polym. Degrad. Stabil.* 1987, **19**, 323
48 Leising, G. *Synth. Met.* 1989, **28**, D215
49 Friend, R. H., Bradley, D. D. C. and Townsend, P. D. *J. Phys. D: Appl. Phys.* 1987, **20**, 1367
50 Leising, G. *Phys. Rev. B.* 1988, **38**, 10303
51 Eckhardt, H. *J. Chem. Phys.* 1983, **79**, 2085
52 Kubo, T., Takezoe, H. and Fukuda, A. *Jpn J. Appl. Phys.* 1991, **30**, L1562
53 Pichler, K., Friend, R. H., Parker, D. and Feast, W. J. *J. Phys.:*

Condensed Matter 1991, **3**, 3007
54 Friend, R. H., Schaffer, H. E., Heeger, A. J. and Bott, D. C. *J. Phys. C: Solid State Phys.* 1987, **20**, 6013
55 Schaffer, H. E., Friend, R. H. and Heeger, A. J. *Phys. Rev. B.* 1987, **36**, 7537
56 Vogl, P. and Campbell, D. K. *Phys. Rev. Lett.* 1989, **62**, 2012
57 Wei, X., Hess, B. C., Vardeny, Z. V. and Wudl, F. *Phys. Rev. Lett.* 1992, **68**, 666
58 Orenstein, J. and Baker, G. L. *Phys. Rev. Lett.* 1982, **49**, 1043
59 Townsend, P. D. and Friend, R. H. *Synth. Met.* 1987, **17**, 361
60 Pichler, K., Gelsen, O. M., Bradley, D. D. C., Friend, R. H., Parker, D. and Feast, W. J. *Springer Ser. Solid State Sci.* 1992, **107**, 238
61 Terai, A. and Ono, Y. *Synth. Met.* 1992, **49–50**, 603
62 Burroughes, J. H., Jones, C. A. and Friend, R. H. *Nature* 1988, **335**, 137
63 Wittmann, J. C. and Smith, P. *Nature* 1991, **352**, 414
64 Pichler, K., Friend, R. H., Burn, P. L. and Holmes, A. B. *Synth. Met.* 1993, **55–57**, 454
65 Harper, K. and James, P. G. *Mol. Cryst. Liq. Cryst.* 1985, **117**, 55